Phosphorylation of paracellin-1 at Ser217 by protein kinase A is essential for localization in tight junctions

Akira Ikari[1,2,*], Satomi Matsumoto[1], Hitoshi Harada[1], Kuniaki Takagi[1], Hisayoshi Hayashi[3], Yuichi Suzuki[3], Masakuni Degawa[4] and Masao Miwa[2]

[1]Department of Environmental Biochemistry and Toxicology, [2]Department of Pharmaco-Biochemistry, School of Pharmaceutical Sciences, [3]Laboratory of Physiology, School of Food and Nutritional Sciences, and [4]Department of Molecular Toxicology and COE Program for the 21st Century, University of Shizuoka, 52-1 Yada, Shizuoka 422-8526, Japan

*Author for correspondence (e-mail: ikari@u-shizuoka-ken.ac.jp)

Accepted 20 January 2006
Journal of Cell Science 119, 1781-1789 Published by The Company of Biologists 2006
doi:10.1242/jcs.02901

Summary

Although paracellin-1 (PCLN-1) is known to have a crucial role in the control of Mg^{2+} reabsorption in the kidney, the molecular pathways involved in the regulation of PCLN-1 have not been clarified. We used FLAG-tagged PCLN-1 to investigate these pathways further, and found that PCLN-1 is phosphorylated at Ser217 by protein kinase A (PKA) under physiological conditions in Madin-Darby canine kidney (MDCK) cells. PCLN-1 expression decreased Na^+ permeability, resulting in a decrease in the transepithelial electrical resistance (TER). By contrast, PCLN-1 enhanced transepithelial Mg^{2+} transport. PKA inhibitors, *N*-[2-(*p*-bromocinnamylamino)ethyl]-5-isoquinolinesulfonamide dihydrochloride (H-89) and myristoylated protein kinase A inhibitor 14-22 amide PKI, and an adenylate cyclase inhibitor, 2′,5′-dideoxy adenosine (DDA), reduced the phosphoserine level of PCLN-1. The inhibitory effect of DDA was rescued by 8-bromoadenosine-3′,5′-cyclic monophosphate (8-Br-cAMP). PKA and adenylate cyclase inhibitors decreased transepithelial Mg^{2+} transport and TER. Dephosphorylated PCLN-1 moved from detergent-insoluble to soluble fractions and was dissociated from ZO-1. A fusion protein of PCLN-1 with glutathione-*S*-transferase revealed that Ser217 was phosphorylated by PKA. Phosphorylated PCLN-1 was localized in the tight junction (TJ) along with ZO-1, whereas dephosphorylated PCLN-1 and the S217A mutant were translocated into the lysosome. The degradation of dephosphorylated PCLN-1 and S217A mutant was inhibited by chloroquine, a specific lysosome inhibitor. Thus, the PKA-dependent phosphorylation of Ser217 in PCLN-1 is essential for its localization in the TJ and transepithelial Mg^{2+} transport.

Key words: Mg^{2+} reabsorption, Phosphorylation, PKA, Tight junction, Lysosome

Introduction

Mg^{2+} is an important cofactor for most of the ATPases. The Mg^{2+} content of an individual is controlled by reabsorption through the renal tubular epithelial cells. The renal Mg^{2+} filtrated in the glomeruli is predominantly reabsorbed by the paracellular pathway in the thick ascending limb of Henle (TAL) (Quamme and de Rouffignac, 2000). Several homozygous mutations in the *paracellin-1* gene have been found in familial hypomagnesemia-hypercalciuria syndrome (Blanchard et al., 2001; Simon et al., 1999; Tasic et al., 2005). Paracellin-1 (PCLN-1) belongs to the claudin family (named claudin-16) and is exclusively expressed in the most apical intercellular junction – the tight junction (TJ) of the TAL. Thus, PCLN-1 appears to function as a paracellular pore for Mg^{2+}.

Madin-Darby canine kidney (MDCK) epithelial cells, derived from the canine renal collecting duct, are widely used as an in vitro model to delineate mechanisms involved in the biogenesis and regulation of the TJ. This cell line forms an epithelial monolayer in culture that contains the functionally intact TJ. The TJ comprises a complex of multiple transmembrane and peripheral proteins including claudins. Claudins consist of a family of at least 24 homologous isoforms and bear four transmembrane domains (Tsukita et al., 1999). The C-terminal tail of claudins has a PDZ-binding motif and can interact with the PDZ domains of zonula occludens proteins ZO-1, ZO-2 and ZO-3. The interactions of these proteins are crucial for the assembly of the TJ and the maintenance of barrier function (Furuse et al., 1994; Itoh et al., 1999a; Wittchen et al., 1999). Furthermore, ZO-1 and ZO-2 bind directly to actin filaments at their C-terminal regions, suggesting that these molecules function as crosslinkers between the TJ strands and actin filaments (Fanning et al., 1998; Itoh et al., 1997; Itoh et al., 1999b; Wittchen et al., 1999).

Details concerning the functional properties of single claudins have been described for claudin-1, -2, -4, -8 and -15. The expression of claudin-1, -4, -8 or -15 in MDCK cells increases transepithelial electrical resistance (TER) (Colegio et al., 2002; McCarthy et al., 2000; Van Itallie et al., 2001; Van Itallie et al., 2003; Yu et al., 2003). Claudin-4 expression reduces the Na^+ permeability and claudin-8 expression reduces the cation permeability. Conversely, the expression of claudin-2 decreases the TER by selectively increasing the permeability to cations (Amasheh et al., 2002). Similarly, knockout or inactivating mutants of claudin genes can cause aberration in the paracellular permeability (Gow et al., 1999; Wilcox et al., 2001). Each isoform exhibits a tissue-specific and segment-

specific pattern of distribution, and determines the various properties of paracellular permeability in different epithelial cells.

We recently reported that PCLN-1 is associated with ZO-1 and is localized in the TJ area in MDCK cells stably expressing FLAG-tagged PCLN-1 (Ikari et al., 2004). PCLN-1 expression leads to an increase in TER and the paracellular transport of divalent cations. However, the regulatory mechanisms of PCLN-1 are still unclear. It has been reported that kinases are involved in the biogenesis and regulation of the several TJ components (Hopkins et al., 2003; Kale et al., 2003; Karczewski and Groot, 2000; Nusrat et al., 2000b). In the present study, we found that PCLN-1 is phosphorylated at Ser217 by protein kinase A (PKA) under physiological conditions, and that phosphorylated PCLN-1 is localized in the TJ. Conversely, dephosphorylated PCLN-1 is dissociated from the TJ and is translocated into the lysosome. Our present results indicate that the phosphorylation of PCLN-1 is essential for paracellular Mg^{2+} transport.

Results

PCLN-1 is phosphorylated by PKA

The expression of FLAG-tagged PCLN-1 in MDCK cells was checked by anti-PCLN-1 and anti-FLAG antibodies (Fig. 1A,B). Mock MDCK cells showed no expression of endogenous PCLN-1. The introduction of PCLN-1 did not affect the endogenous expression of occludin, claudin-1 and claudin-4, TJ integral membrane proteins, or the TJ scaffolding protein ZO-1 (Fig. 1C-F). PCLN-1 was constitutively phosphorylated in the unstimulated cells (Fig. 1H). PKA inhibitors, *N*-[2-(p-bromocinnamylamino)ethyl]-5-isoquinolinesulfonamide (H-89) and myristoylated protein kinase A inhibitor 14-22 amide (PKI), and an adenylate cyclase inhibitor, 2′,5′-dideoxy adenosine (DDA), decreased the phosphoserine level of PCLN-1 without decreasing the amount of PCLN-1 expression (Fig. 1G-J). 8-Bromoadenosine-3′,5′-cyclic monophosphate (8-Br-cAMP) rescued the phosphoserine level of PCLN-1 that had been decreased by DDA. These results support the view that PCLN-1 is phosphorylated by a cAMP/PKA-dependent pathway under physiological conditions. Similarly, it has been reported that claudin-3 is phosphorylated in unstimulated ovarian cancer cells (D'Souza et al., 2005).

PCLN-1 expression decreases Na^+ permeability

The epithelial TJ shows ions and size selectivity, and their barrier function varies significantly in tightness depending on the cell type and physiological requirements (Anderson, 2001; Balda et al., 1996). TER values of PCLN-1-expressing MDCK cells were increased relative to mock cells (Fig. 2A). The increase in TER induced by PCLN-1 could result from a selective or nonselective decrease in permeability for cations and anions. Similar to the previous reports (Kahle et al., 2004; Van Itallie et al., 2001; Yu et al., 2003), mock MDCK cells showed higher absolute permeability for Na^+ (P_{Na}) than Cl^- (P_{Cl}) (Fig. 2B). PCLN-1 decreased P_{Na}/P_{Cl} with decrease in the dilution potential. The values of the dilution potential in mock and PCLN-1-expressing MDCK cells were 9.68±0.58 mV and 7.37±0.47 mV (n=9), respectively. We found that this decrease was attributed to a decrease in the Na^+ permeability (Fig. 2C).

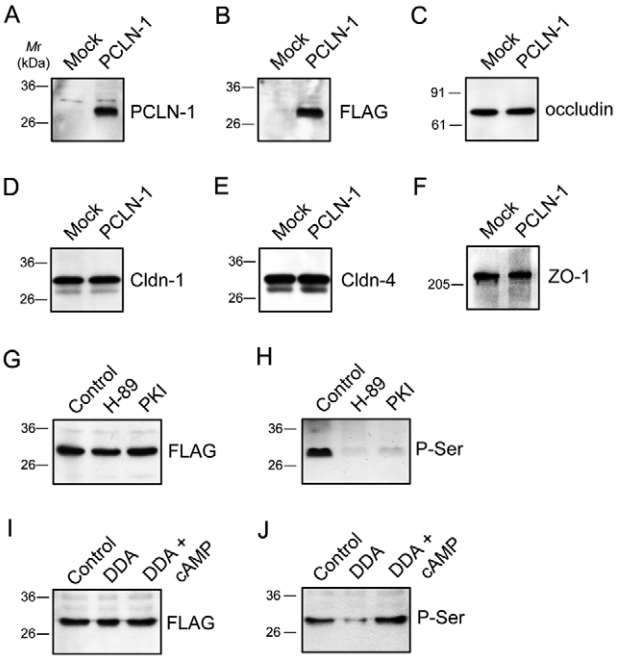

Fig. 1. Phosphorylation of paracellin-1 by cAMP. (A-F) Whole membrane fractions were prepared from MDCK cells expressing FLAG (Mock) or FLAG-tagged PCLN-1 (PCLN-1). The fractions (30 μg) were applied to SDS-polyacrylamide gel and then immunoblotted with antibodies raised against PCLN-1 (A), FLAG (B), occludin (C), claudin-1 (D), claudin-4 (E) or ZO-1 (F). To quantify the expression levels of these proteins, the amounts of occludin, claudin-1, claudin-4 and ZO-1 in the mock cells were normalized as 100%. In the PCLN-1-expressing cells, the relative expression levels of occludin, claudin-1, claudin-4 and ZO-1 were 98.6±8.5% (n=4), 104±4.1% (n=6), 102±9.0% (n=6) and 98.2±2.5% (n=4), respectively. (G-J) MDCK cells expressing FLAG-tagged PCLN-1 were treated with 50 μM H-89, 10 μM PKI or 50 μM DDA for 1 hour. When used, 100 μM 8-Br-cAMP (cAMP) was treated for 1 hour after the addition of DDA. Whole membrane fractions (30 μg) were immunoblotted with anti-FLAG antibody (G,I). The whole membrane fractions (500 μg) were incubated with protein G-Sepharose and anti-FLAG antibody. The immune pellets were immunoblotted with anti-phosphoserine (P-Ser) antibody (H,J).

Dephosphorylation of PCLN-1 decreases TER and transepithelial Mg^{2+} transport

In PCLN-1-expressing MDCK cells, the PKA inhibitors H-89 and PKI, and the adenylate cyclase inhibitor DDA, decreased TER (Fig. 3A). These inhibitors had no effect on the flux of FITC-dextran-4k, which is a non-ionic molecule (Fig. 3B). Transepithelial Mg^{2+} transports of PCLN-1-expressing cells from the apical to basal compartments were higher than those of mock cells (Fig. 3C), indicating that PCLN-1 acts as a Mg^{2+}-permeable pore. PKA inhibitors decreased transepithelial Mg^{2+} transport of PCLN-1-expressing cells to the same level as mock cells (Fig. 3D). Similar to the effect on TER, 8-Br-cAMP completely rescued the DDA-induced decrease in transepithelial Mg^{2+} transport. In mock cells, PKA inhibitors and 8-Br-cAMP had no effect on TER, the FITC-dextran-4k flux or transepithelial Mg^{2+} transport. These results suggest that PKA inhibitors block the functions of PCLN-1 as a transepithelial barrier and Mg^{2+} transporter.

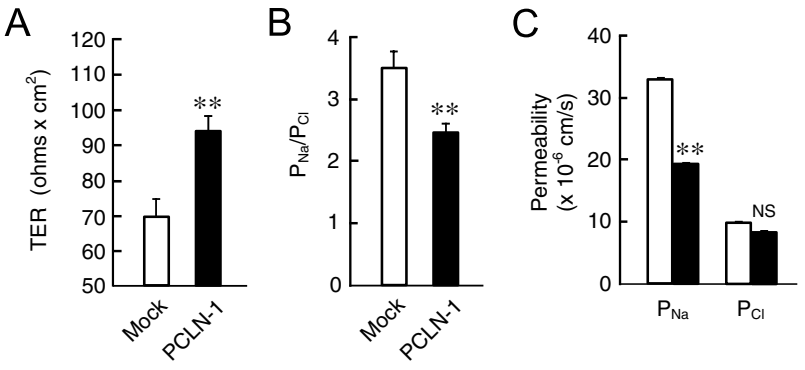

Fig. 2. Effects of PCLN-1 expression on paracellular permeability. (A) Mock (open columns) and FLAG-tagged PCLN-1-expressing MDCK cells (closed columns) were plated on Snapwell polyester filters. TER values were measured at 7 days after plating. (B,C) Mock (open columns) and FLAG-tagged PCLN-1-expressing cells (closed columns) were cultured for 7 days. The absolute permeability for Na^+ (P_{Na}) and Cl^- (P_{Cl}) and relative permeability of Na^+ to Cl^- (P_{Na}/P_{Cl}) were calculated as described in the Materials and Methods. $^{**}P<0.01$, compared with mock cells. NS, not significant compared with mock cells.

PCLN-1 is distributed in the detergent-insoluble fractions

The TJ proteins were mainly distributed in the Triton X-100-insoluble fractions under physiological conditions (Nusrat et al., 2000a). PCLN-1 was distributed in the Triton X-100-insoluble fractions in MDCK cells (Fig. 4A). PKA inhibitors led PCLN-1 to become more soluble in the Triton X-100-containing solution. DDA also increased the amount of PCLN-1 in the Triton X-100-soluble fractions and 8-Br-cAMP restored PCLN-1 to the Triton X-100-insoluble fractions. The qualitative change in the PCLN-1 distribution pattern probably represents an alteration in the association of PCLN-1 with the actin-based cytoskeleton.

PCLN-1 is associated with ZO-1 in the TJ area

The direct binding of ZO-1 with the C-terminus (TRV sequence) of PCLN-1 has been revealed with an in vitro binding assay using a glutathione-*S*-transferase (GST) fusion protein and in vivo immunoprecipitation analysis (Ikari et al., 2004; Müller et al., 2003). ZO-1 forms crosslinks between the TJ strand and actin-based cytoskeleton. H-89, PKI and DDA had no effects on the endogenous expression of ZO-1 (Fig. 4B). However, the association of PCLN-1 with ZO-1 was diminished by H-89, PKI and DDA. 8-Br-cAMP restored the association of PCLN-1 with ZO-1 invalidated by DDA treatment. These results suggest that the phosphorylation of PCLN-1 is necessary for it to associate with ZO-1 and cytoskeletal proteins. Similarly, PCLN-1 was co-localized with ZO-1 in the TJ of MDCK cells under physiological conditions (Fig. 5). The x-z-scan images showed that merged yellow spots appeared near the most apical regions in the control cells. H-89, PKI and DDA caused PCLN-1 to be distributed in the cytoplasmic region. By contrast, the localization of ZO-1 was not disturbed by these inhibitors as compared with the control cells. 8-Br-cAMP recovered the tight junctional localization of PCLN-1 disturbed by DDA. These results suggest that the cAMP/PKA-dependent pathway directly regulates the localization of PCLN-1 in the TJ without affecting the anchoring protein ZO-1.

Ser217 of PCLN-1 is phosphorylated by PKA

The amino acid sequences of PCLN-1 are well preserved among mammals. Rat PCLN-1 shows 91, 88 and 99% identities with human, bovine and mouse homologs, respectively (Weber et al., 2001). PCLN-1 contains 12 serine

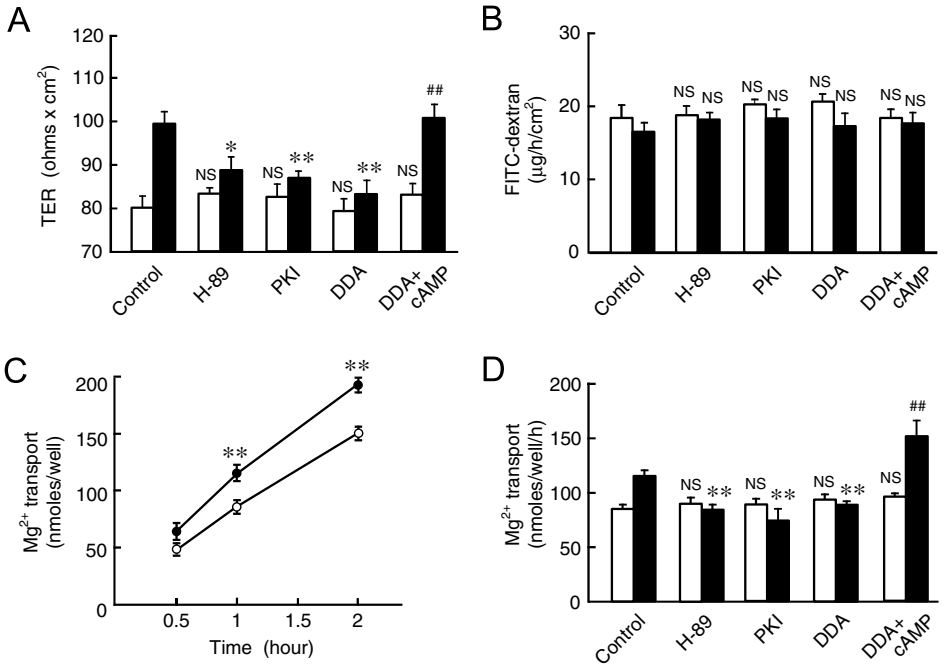

Fig. 3. Effects of PKA inhibitors on paracellular permeability. (A,B,D) Mock (open columns) and FLAG-tagged PCLN-1-expressing MDCK cells (closed columns) were treated with 50 μM H-89, 10 μM PKI or 50 μM DDA for 1 hour. When used, 100 μM 8-Br-cAMP (cAMP) was treated for 1 hour after the addition of DDA. TER, FITC-dextran-4k flux and Mg^{2+} transport from the apical to basal compartments were measured after treatment with each drug. $^{*}P<0.05$ and $^{**}P<0.01$, compared with control. $^{\#\#}P<0.01$, compared with DDA only. NS, not significant compared with the control. (C) Mg^{2+} transport from the apical to basal compartments was measured in mock (open circles) and FLAG-tagged PCLN-1-expressing MDCK cells (closed circles). After incubation at 37°C for 0.5, 1 or 2 hours, the basal compartment media were collected and subjected to Mg^{2+} measurement. $^{**}P<0.01$, compared with mock cells.

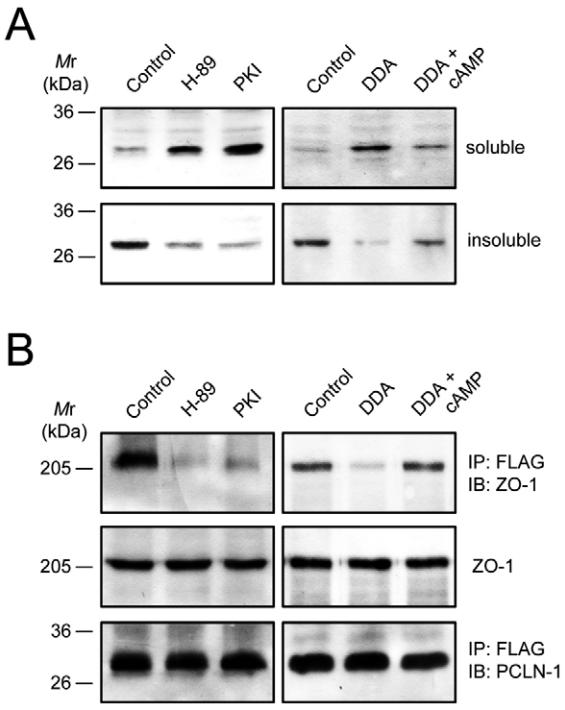

Fig. 4. Effects of PKA inhibitors on PCLN-1 distribution. Mock and FLAG-tagged PCLN-1-expressing MDCK cells were treated with 50 μM H-89, 10 μM PKI, 50 μM DDA or 50 μM DDA for 1 hour. When used, 100 μM 8-Br-cAMP (cAMP) was treated for 1 hour after the addition of DDA. (A) The Triton X-100-soluble (60 μg) and -insoluble fractions (30 μg) were immunoblotted with anti-FLAG antibody. (B) The whole membrane fractions (500 μg) were incubated with protein G-Sepharose and anti-FLAG antibody to immunoprecipitate (IP). The immune pellets were immunoblotted (IB) with anti-ZO-1 antibody (upper) or anti-PCLN-1 (lower) antibodies. Whole membrane fractions (30 μg) were immunoblotted with anti-ZO-1 antibody (middle).

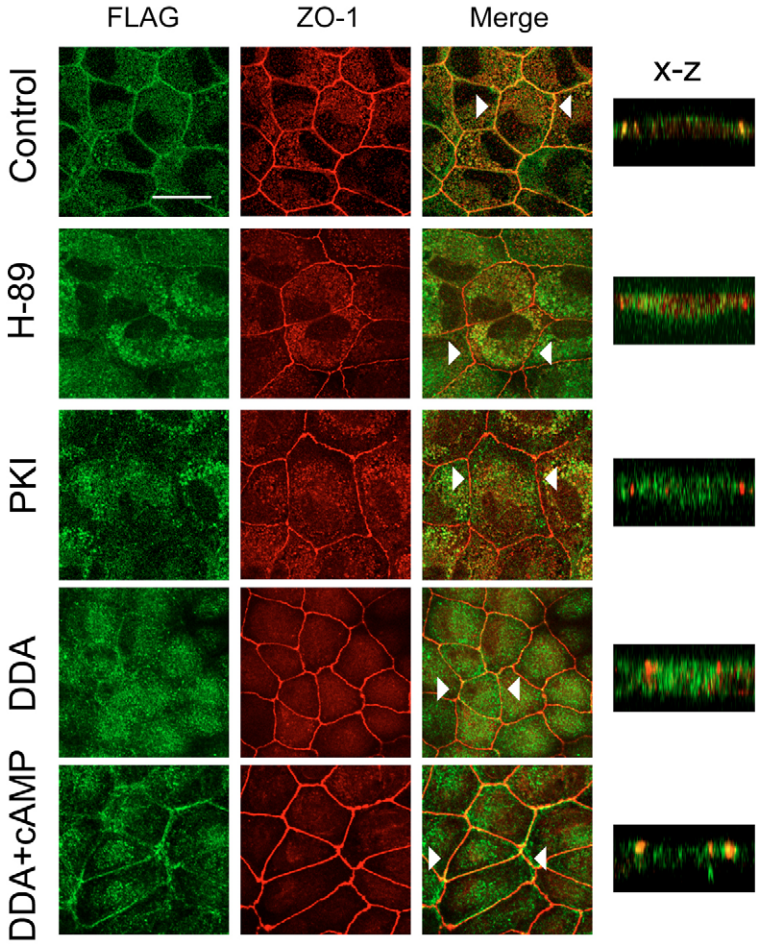

Fig. 5. Localization of PCLN-1 in the TJ. FLAG-tagged PCLN-1-expressing MDCK cells were treated with 50 μM H-89, 10 μM PKI, 50 μM DDA or 50 μM DDA for 1 hour. When used, 100 μM 8-Br-cAMP (cAMP) was treated for 1 hour after the addition of DDA. Cells were double stained with anti-FLAG antibody (green) and anti-ZO-1 antibody (red). The x-y sections represent the area of the TJ. Right panels (x-z) show the vertical sections indicated by the triangles at the merged images. Bar, 10 μm.

residues and, among them, Ser208, Ser213 and Ser217 of the rat homologs are located in the cytoplasmic space (Fig. 6A). These three serine residues are fully conserved in the mammalian PCLN-1s. The cytoplasmic C-terminal domain of PCLN-1 was expressed as a fusion protein with GST, and immobilized on glutathione-Sepharose 4B beads (Fig. 6B). The S208A and S213A mutants, as well as wild-type (WT) PCLN-1, were phosphorylated by active PKA subunits, but the S217A mutant was not. Our point substitution studies indicated that Ser217 is a crucial residue in the phosphorylation of PCLN-1 by PKA. These results are in agreement with the prediction by the database on the NetPhos 2.0 Server (http://www.cbs.dtu.dk/services/NetPhos/).

To examine the function of the S217A mutant, we constructed MDCK cells stably expressing the S217A mutant PCLN-1. The amount of S217A mutant protein was equal to that of the WT PCLN-1 (Fig. 6C). The expression of S217A mutant PCLN-1 had no effect on the endogenous expressions of claudin-1 and claudin-4 (Fig. 6D,E). In contrast to WT PCLN-1, the S217A mutant was largely dephosphorylated under physiological conditions (Fig. 6F). In common with WT PCLN-1 treated with PKA inhibitors (Fig. 4A,B), the S217A protein was mainly distributed in the Triton X-100-soluble fraction (Fig. 6G) and was dissociated from ZO-1 (Fig. 6H). TER, the flux of FITC-dextran-4k and the Mg^{2+} transport of the S217A mutant were not significantly different from those of the mock cells (Fig. 6I-K), indicating that the phosphorylation of Ser217 in PCLN-1 is necessary to carry out its functions.

Dephosphorylated PCLN-1 is translocated into the lysosome

To examine the subcellular localization of PCLN-1, we performed double immunofluorescence confocal microscopy analysis of PCLN-1 and organelle markers. Fig. 7A shows that WT PCLN-1 did not overlap with lysosomes (lysotracker), Golgi (furin) or early endosomes (early endosomal antigen 1). Conversely, WT PCLN-1 treated with H-89 was co-localized

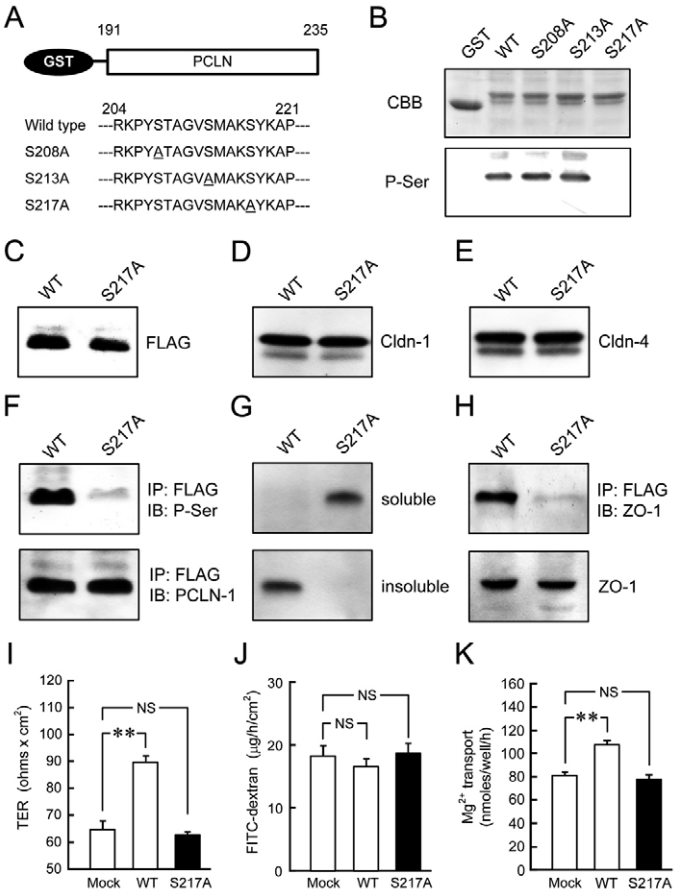

Fig. 6. Dysfunction of PCLN-1 by the S217A mutation. (A) Schematic description of the GST-fused cytoplasmic C-terminal domain of PCLN-1. (B) Proteins were fractionated on gels and stained with Coomassie Brilliant Blue (CBB) for the detection of GST proteins. The proteins bound to beads were incubated with the activated PKA subunit, and were then immunoblotted with anti-phosphoserine antibody (P-Ser). (C-E) Whole membrane fractions (30 μg) were immunoblotted with anti-FLAG (C), anti-claudin-1 (D) or anti-claudin-4 antibodies (E). As compared with cells expressing WT PCLN-1, the relative expression levels in cells expressing the S217A mutant PCLN-1 were 102±6.0% (claudin-1) and 97.1±9.0% (claudin-4), respectively. (F,H) Whole membrane fractions (500 μg) were incubated with protein G-Sepharose and anti-FLAG antibody to immunoprecipitate (IP). The immune pellets were immunoblotted (IB) with (F, upper) anti-phosphoserine (P-Ser), (F, lower) anti-PCLN-1, or (H, upper) anti-ZO-1 antibodies. Whole membrane fractions (30 μg) were immunoblotted with anti-FLAG or anti-ZO-1 antibodies (H, lower). (G) The Triton X-100-soluble (60 μg) and -insoluble fractions (30 μg) were immunoblotted with anti-FLAG-antibody. (I-K) TER, FITC-dextran-4k flux and Mg^{2+} transport were measured in MDCK cells expressing FLAG (Mock), FLAG-tagged WT PCLN-1 (WT), or FLAG-tagged S217A mutant PCLN-1 (S217A). $^{**}P<0.01$. NS, not significant.

with lysotracker (Fig. 7B). The S217A mutant, a non-phosphorylated mutant of PCLN-1, was distributed in the cytoplasmic region far from the TJ and was co-localized with lysotracker (Fig. 7C). In most cases, the lysosomal pathway is involved in the degradation of proteins. In the presence of cycloheximide, a protein synthesis inhibitor, H-89 decreased the expression of PCLN-1 (Fig. 8A, middle). Similarly, the expression of S217A mutant PCLN-1 was decreased by cycloheximide (Fig. 8B, middle). The expression of ZO-1 was not affected by cycloheximide (Fig. 8A,B, upper). These results suggest that dephosphorylated and non-phosphorylated PCLN-1 might be degraded by proteases. The decrease of PCLN-1 expression was inhibited by chloroquine, a specific lysosome inhibitor (Ohkuma et al., 1986), but not by lactacystin, a specific proteasome inhibitor (Dick et al., 1996). Furthermore, a new band was detected at about 38 kDa by the treatment with chloroquine. These results indicate that the dephosphorylated and non-phosphorylated PCLN-1 are translocated to the lysosome and are degraded by lysosomal proteases. The lysosomal pathway is involved in the degradation of ubiquitylated proteins (Marques et al., 2004). Therefore, we examined whether dephosphorylated and non-phosphorylated PCLN-1 were ubiquitylated in the present conditions. In immunoprecipitation by anti-FLAG antibody, ubiquitylated protein was detected at about 38 kDa (Fig. 8A,B, lower). The apparent molecular mass of ubiquitylated protein is compatible with mono-ubiquitylation of PCLN-1. We suggest that the phosphorylation of PCLN-1 can inhibit ubiquitylation under physiological conditions and thereby protect itself against internalization and degradation.

Discussion

The renal Mg^{2+} filtrated in the glomeruli is predominantly reabsorbed by the paracellular pathway in the TAL (Quamme, 1989). Renal Mg^{2+} homeostasis is controlled by the reabsorption pathway because significant Mg^{2+} secretion has not been reported in the tubule segments. The molecule responsible for the paracellular Mg^{2+} transport pathway has remained unidentified. We recently reported that the expression of PCLN-1 leads to an increase in the paracellular transport of divalent cations according to the transepithelial potential. In the present study, we found that PCLN-1 is phosphorylated by PKA under physiological conditions and that the phosphorylation is necessary for the localization of PCLN-1 in the TJ and for transepithelial Mg^{2+} transport.

Hypermagnesemia induces a decrease in the urinary excretion of cAMP and the reabsorption of Mg^{2+} in the TAL (Quamme, 1997; Slatopolsky et al., 1976). Conversely, the reabsorption of Mg^{2+} is increased by cAMP-generating hormones, such as arginine vasopressin, parathyroid hormone and glucagon (Wittner and Di Stefano, 1990), suggesting that the reabsorption of Mg^{2+} is positively regulated by cAMP. Transepithelial Mg^{2+} reabsorption is passive diffusion according to the positive luminal transepithelial potential (Mandon et al., 1993). The voltage in the lumen of the TAL is determined by the rate of the Na^+-K^+-Cl^- cotransporter, the apical K^+ channel and the basal Na^+/K^+-ATPase (Greger, 1985; Quamme, 1989). The Na^+-K^+-Cl^- cotransporter and Na^+/K^+-ATPase are positively regulated by a cAMP/PKA-dependent pathway (Kiroytcheva et al., 1999; Meade et al., 2003). PKA inhibitors might indirectly block transepithelial Mg^{2+} transport mediated by the inhibition of the Na^+-K^+-Cl^- cotransporter or Na^+/K^+-ATPase. However, this possibility is contradicted by the results that the S217A mutant, which is not phosphorylated by PKA, had no effect on TER and transepithelial Mg^{2+} transport without treatment with PKA inhibitors (Fig. 6).

Recently, Hou et al. reported that PCLN-1 leads to a large increase in Na^+ permeability and a small increase in Mg^{2+}

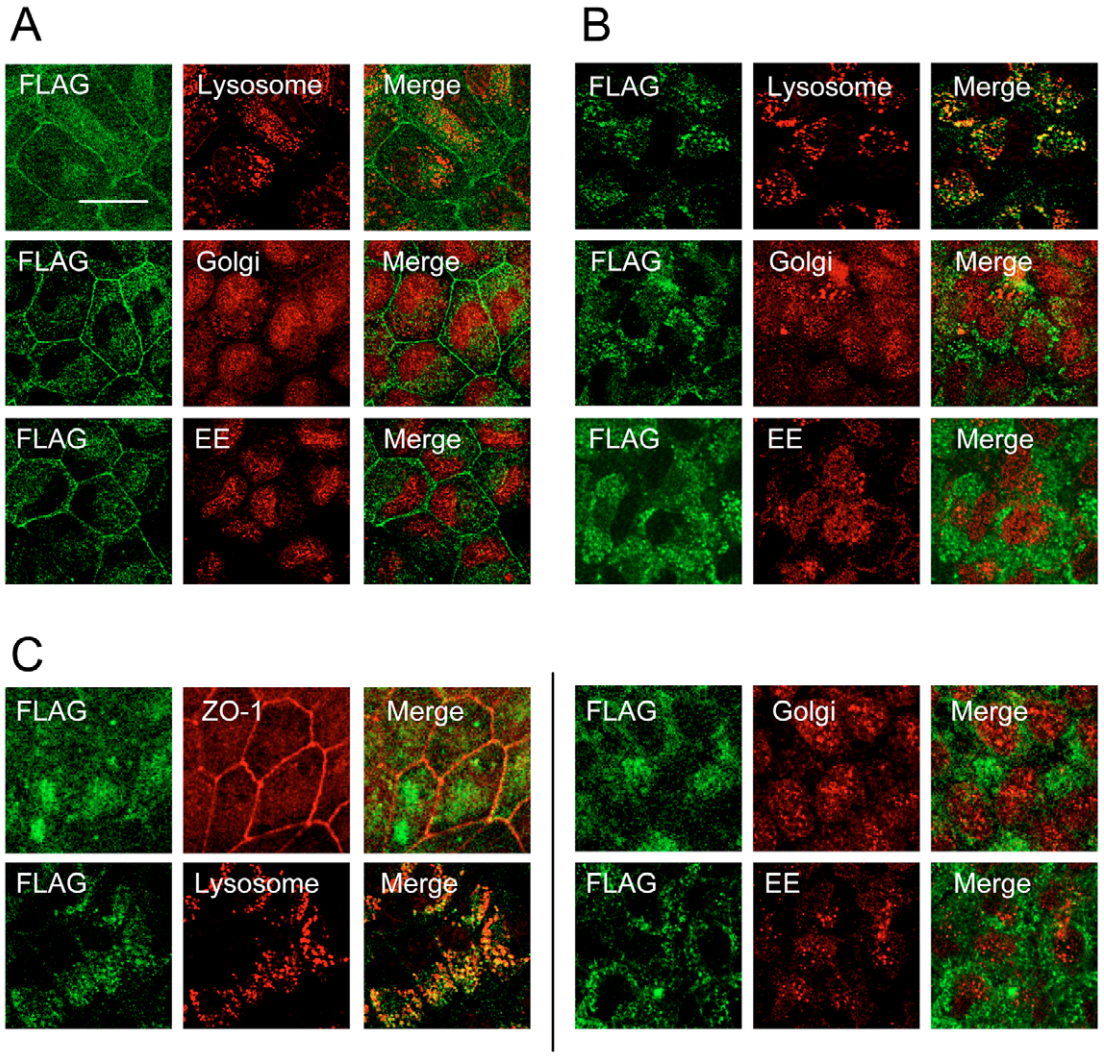

Fig. 7. Lysosomal targeting of PCLN-1 by dephosphorylation. (A,B) MDCK cells expressing WT PLCN-1 were grown to a confluent condition on cover glasses. Cells were incubated in the absence (A) and presence (B) of 50 μM H-89 for 1 hour. The cells were then double stained with anti-FLAG antibody (green) and organelle markers (red) of lysosomes (lysotracker), Golgi (furin) or early endosomes (EE, early endosomal antigen 1). (C) MDCK cells expressing the S217A mutant PCLN-1 were double stained with anti-FLAG antibody (green) and ZO-1 (red) or organelle markers (red) of lysosomes, Golgi or EE. The x-y sections represent the area of the TJ. Bar, 10 μm.

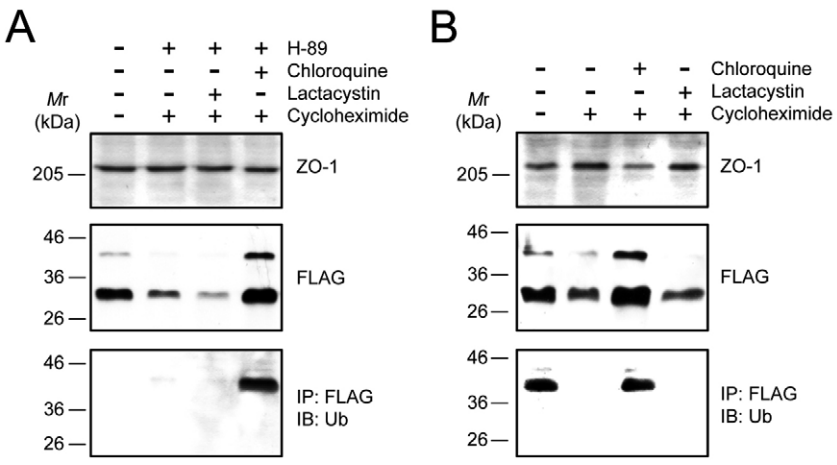

Fig. 8. Degradation of dephosphorylated PCLN-1 in the lysosome. (A) MDCK cells expressing WT PLCN-1 were treated with 50 μM H-89, 50 μM H-89 plus 10 μM lactacystin, or 50 μM H-89 plus 100 μM chloroquine for 3 hours in the presence of 10 μM cycloheximide. (B) MDCK cells expressing the S217A mutant PLCN-1 were treated with 10 μM lactacystin or 100 μM chloroquine for 3 hours in the presence of 10 μM cycloheximide. Whole membrane fractions (30 μg) were immunoblotted with anti-ZO-1 (A,B, upper) or anti-FLAG antibody antibodies (A,B, middle). The whole membrane fractions (500 μg) were incubated with protein G-Sepharose and anti-FLAG antibody to immunoprecipitate (IP). The immune pellets were immunoblotted (IB) with anti-ubiquitin antibody (Ub; A,B, lower).

permeability in LLC-PK$_1$ cells (Hou et al., 2005). In the present study, we found that PCLN-1 decreases Na^+ permeability and increases Mg^{2+} transport in MDCK cells. At present, we do not know why PCLN-1 causes contradictory effects on Na^+ permeability in LLC-PK$_1$ and MDCK cells. Thus, further study is needed to clarify how PCLN-1 changes Na^+ permeability.

To date, other claudins have been reported to be phosphorylated by protein kinases. Claudin-1 and claudin-4 are phosphorylated by PKC (D'Souza et al., 2005; Nunbhakdi-Craig et al., 2002). Claudin-3 and claudin-5 are phosphorylated by PKA (D'Souza et al., 2005; Soma et al., 2004). In addition, protein kinase WNK4 has been shown to phosphorylate claudin-1, -2, -3 and -4 (Yamauchi et al., 2004). Different phosphorylation mechanisms must operate predominantly in different types of claudins. There are no reports of whether the phosphorylation level of PCLN-1 (claudin-16) is involved either in its expression and/or in its function as a transepithelial barrier and Mg^{2+} transporter. Treatment with PKA inhibitors for 1 hour did not change the expression level of PCLN-1 protein, indicating that PKA inhibitors have no effect on the transcriptional and translational steps of PCLN-1 in the present experimental conditions. Dephosphorylation of PCLN-1 by PKA inhibitors induced a decrease in TER and transepithelial Mg^{2+} transport without affecting diffusion of FITC-dextran-4k (Fig. 3). This is the first report showing that the PKA-dependent phosphorylation of PCLN-1 is necessary to carry out its functions.

The detergent insolubility of proteins is considered to indicate their integration into the macromolecular complex. The TJ proteins make a continuous anastomosing network of intramembranous particle strands and are associated with actin filaments (Staehelin, 1974). Therefore, transmembrane TJ proteins are resistant to detergent extraction. Our results indicate that phosphorylated PCLN-1 is present in the Triton X-100-insoluble fractions, whereas dephosphorylated PCLN-1 is mostly present in the Triton X-100-soluble fractions (Fig. 4A). Similarly, Fujibe et al. reported that the phosphorylation of claudin-1 is involved in its corporation into the TJ and promotion of TJ functions (Fujibe et al.. 2004). Dephosphorylated PCLN-1, which was induced by PKA and adenylate cyclase inhibitors, was dissociated from ZO-1 and was distributed in the cytoplasmic areas (Fig. 4B, Fig. 5), indicating that phosphorylation of PCLN-1 is necessary for anchoring it to the TJ area.

PKA inhibitors might affect other claudins or the TJ-associated proteins, such as ZO-1 and ZO-2. ZO-2 has been shown to be phosphorylated by PKA, affecting its function at the junctional complex (Avila-Flores et al., 2001). However, it was noted that the S217A mutant, which is not phosphorylated by PKA, was dissociated from ZO-1 and was distributed in the cytoplasmic area without the treatment of PKA inhibitors (Figs 6 and 7). The cAMP/PKA-dependent pathway must directly regulate the localization of PCLN-1 in the TJ mediated by phosphorylation at Ser217. Similarly, the localization of claudin-5 in the TJ is upregulated by PKA-induced phosphorylation in endothelial cells (Ishizaki et al., 2003). By contrast, D'Souza et al. reported that claudin-3 is diffused from the TJ to other membrane or cytoplasmic areas by PKA-dependent phosphorylation (D'Souza et al., 2005). Further study is needed to clarify why claudins phosphorylated by PKA are translocated in opposite directions: PCLN-1 (claudin-16) and claudin-5 are translocated to the TJ, whereas claudin-3 is translocated to the cytoplasmic area.

The lysosome is responsible for the degradation of membrane or extracellular proteins that enter the cells by endocytosis. In most cases, the lysosomal pathway is involved in the degradation of ubiquitylated proteins (Marques et al., 2004). The process is divided into two pathways: poly-ubiquitylation, the attachment of multimeric chains of ubiquitin; and mono-ubiquitylation, the attachment of a single ubiquitin. Chimeras consisting of mono-ubiquitin fused to the cytoplasmic regions of the invariant chain of the interleukin-2 receptor α chain (Mosesson et al., 2003) or epidermal growth factor receptor (Nakatsu et al., 2000) are constitutively internalized from the cell surface and targeted to the late endosomal/lysosomal compartment, indicating that a single ubiquitin molecule carries both internalization and sorting signals. PCLN-1 was ubiquitylated under the conditions of dephosphorylation and non-phosphorylation (Fig. 8). Similarly, dephosphorylated protein kinase C isozymes, PKCα and ϵ, undergo ubiquitylation and proteolytic degradation (Leontieva and Black, 2004). By contrast, PKCδ requires phosphorylation for ubiquitin/proteasome-dependent degradation (Srivastava et al., 2002). These results suggest that the ubiquitylation of phosphoproteins or dephosphopoteins depends on the nature of the protein.

Dynamic regulation of PCLN-1 localization by the cAMP/PKA-dependent pathway provides long-term regulation of the paracellular Mg^{2+} reabsorption in the TAL. Phosphorylated PCLN-1 is localized in the TJ area and behaves as a barrier perforated with a Mg^{2+}-permeable pore. Dephosphorylated PCLN-1 sustains internalization and degradation in the lysosome. Non-phosphorylated PCLN-1 is also translocated to the lysosome. Thus, phosphorylation of PCLN-1 must be necessary to maintain physiological Mg^{2+} reabsorption.

Materials and Methods

Cell culture and transfection

Cell culture and transfection procedures for MDCK cells were described previously (Ikari et al., 2004). The S217A mutation of PCLN-1 was generated using a QuickChange site-directed mutagenesis kit (Stratagene). Stable transfectants of wild-type (WT) or S217A mutant PCLN-1 were maintained in the continuous presence of the selecting drug (0.5 mg/ml G418). At least three stable cell lines were generated for each construct. For the experiments, all cells were generally cultured for 7 days, except where otherwise indicated.

Preparation of membrane fraction and immunoprecipitation

Confluent MDCK cells were scraped into cold phosphate-buffered saline (PBS) and were precipitated by centrifugation. The cells were then lysed in a RIPA buffer containing 150 mM NaCl, 0.5 mM EDTA, 1% Triton X-100, 50 mM Tris-HCl (pH 8.0), a protease inhibitor cocktail (Sigma), and 1 mM phenylmethylsulfonyl fluoride, and were sonicated for 20 seconds. After centrifugation at 1000 ***g*** for 5 minutes, the supernatants were collected (whole membrane fractions). The whole membrane fractions (500 μg) were incubated with protein G-Sepharose beads and the indicated primary antibodies at 4°C for 2 hours with gentle rocking. After centrifugation at 6000 ***g*** for 1 minute, the pellet was washed four times with a RIPA buffer. The whole membrane fractions and immunoprecipitates were solubilized in a sample buffer for SDS-PAGE. Protein concentrations were measured using the protein assay kit (Bio-Rad Laboratories) with bovine serum albumin as the standard.

Western blotting

Western blotting was performed with commercial antibodies raised against FLAG, phosphoserine (Sigma), PCLN-1, occludin (Santa Cruz), ubiquitin (Stressgen Bioreagents), claudin-1, claudin-4 and ZO-1 (Zymed Laboratories). Specific binding of antibodies was detected with peroxidase-conjugated secondary antibodies and visualized by enhanced chemiluminescence detection (Amersham Biosciences).

Measurement of paracellular permeability

MDCK cells were plated at confluent densities on 0.33 cm^2 Snapwell polyester filters (Corning Life Sciences). TER was measured three times per well using a Millicell-ERS epithelial volt-ohmmeter (Millipore), and averaged values were collected. TER values (ohms × cm^2) were normalized according to the area of the monolayer and were calculated by subtracting the blank values from the filter and the bathing medium. In the previous study, we confirmed that TER values reached a maximum at 3 days after plating and declined to a steady state over 7 days (Ikari et al., 2004). Here, we compared the steady-state TER values among mock, the PCLN-1-expressing and the S217A mutant PCLN-1-expressing cells. Paracellular diffusion of FITC-dextran-4k from apical to basal compartments was measured with a Fluoroskan Ascent CF (Thermo Labosystems). The transepithelial transport of Mg^{2+} from the apical to basal compartments was measured using Xylidyl Blue-I (XB-I). At time 0, the transport buffer (140 mM NaCl, 5.8 mM KCl, 0.34 mM Na_2HPO_4, 0.44 mM KH_2PO_4, 1 mM $CaCl_2$, 25 mM glucose and 20 mM Hepes, pH 7.4) supplemented with 10 mM $MgCl_2$ was poured into the filter well and the reverse compartment was filled with the transport buffer without $MgCl_2$. After incubation at 37°C for 0.5, 1 or 2 hours, the reverse compartment media were collected and subjected to Mg^{2+} measurement. XB-I formed a 520 nm absorbance maximum complex upon Mg^{2+} binding under alkaline conditions.

Electrophysiological studies with Ussing chambers

MDCK cells were plated at confluent densities on 1 cm^2 Snapwell polyester filters. The filter rings were then detached and mounted in Ussing chambers that were incubated in buffer A (145 mM NaCl, 5 mM KCl, 1.2 mM $CaCl_2$, 1 mM $MgCl_2$, 10 mM glucose and 10 mM Hepes, pH 7.4) at 37°C. The fluid volume on each side of the filter was 4 ml. Dilution potentials were measured when buffer B (72.5 mM NaCl, 145 mM mannitol, 5 mM KCl, 1.2 mM $CaCl_2$, 1 mM $MgCl_2$, 10 mM glucose and 10 mM Hepes, pH 7.4) was replaced with buffer A on the apical side or basal side of the filters. Electrical potentials obtained from blank inserts were subtracted from those obtained from inserts with the confluent growth of cells. Dilution potentials were identical in magnitude in both the apical and basal directions. The ion permeability ratio (η) for the monolayer was calculated from the dilution potential using the Goldman-Hodgkin-Katz equation, as described elsewhere (Kahle et al., 2004). The absolute permeabilities of Na^+ (P_{Na}) and Cl^- (P_{Cl}) were calculated using a simplified Kimizuka-Koketsu equation (Kimizuka and Koketsu, 1964), $P_{Na}=(G/C)(RT/F^2)\eta/(1+\eta)$ and $P_{Cl}=(G/C)(RT/F^2)/(1+\eta)$, where η is the ratio of permeability of the monolayer to Na^+ over the permeability to Cl^- ($\eta=P_{Na}/P_{Cl}$), G is conductance per unit of surface area, C is the NaCl concentration, R is the gas constant and F is the Faraday constant.

Extraction of MDCK cells with detergent solution

MDCK cells expressing PCLN-1 were subjected to an extraction protocol described previously (Tsukamoto and Nigam, 1997). Extractions were performed by overlaying the cells with CSK-1 buffer (0.5% Triton X-100, 100 mM NaCl, 300 mM sucrose and 10 mM Tris-HCl, pH 7.4) for 30 minutes at 4°C on a gentle rocking platform. The extracts were completely collected (Triton X-100-soluble fractions) and the residue was dissolved in a RIPA buffer. The suspensions were sonicated for 20 seconds and centrifuged at 1000 ***g*** for 5 minutes. The supernatants were referred to as Triton X-100-insoluble fractions.

Confocal microscopy

MDCK cells were grown on cover glasses and, if necessary, were preincubated with a Lysotracker for 30 minutes at 37°C. Immunofluorescence was performed as described previously (Ikari et al., 2004). Immunolabeled cells were visualized on an LSM 510 confocal microscope (Carl Zeiss, Germany) set with the appropriate filter for Texas Red (543 nm excitation, 585-615 nm emission filter) and FITC (488 nm excitation, 530 nm emission filter). Images were collected at increments of 1.0 μm (vertical direction) beginning at the basal membrane and ending at the apical membrane. Images were further processed using Adobe Photoshop (Adobe Systems).

Pull-down and in vitro phosphorylation assay

Escherichia coli BL21 was transformed with plasmids encoding glutathione-*S*-transferase (GST)-fused WT-PCLN-1 (residues 191-235), S208A-PCLN-1, S213A-PCLN-1 and S217A-PCLN-1. GST-fusion proteins were purified with glutathione-Sepharose 4B beads (Amersham Biosciences). Phosphorylation reactions were performed in 50 μl of 20 mM Tris-HCl (pH 7.4) containing 150 mM NaCl, 5 mM $MgCl_2$, 100 μg of GST-fusion proteins, 0.2 mM ATP and 20 U/ml of the PKA catalytic subunit. After incubation for 60 minutes at 30°C, the beads were precipitated by centrifugation. Bound proteins were then eluted with a sample buffer for SDS-PAGE.

Statistics

Results are presented as means ± s.e.m. Differences between groups were analyzed by one-way analysis of variance, and correction for multiple comparison was made using Tukey's multiple comparison test. Comparison between two groups was made using Student's *t* test. Significant differences were assumed at $P<0.05$.

This work was supported in part by the Ministry of Education, Science, Sports and Culture of Japan, a Grant-in-Aid for Encouragement of Young Scientists (to A.I.), and by the grants from The Ichiro Kanehara Foundation, The Salt Science Research Foundation (No. 0525) and Takeda Science Foundation.

References

Amasheh, S., Meiri, N., Gitter, A. H., Schöneberg, T., Mankertz, J., Schulzke, J. D. and Fromm, M. (2002). Claudin-2 expression induces cation-selective channels in tight junctions of epithelial cells. *J. Cell Sci.* **115**, 4969-4976.

Anderson, J. M. (2001). Molecular structure of tight junctions and their role in epithelial transport. *News Physiol. Sci.* **16**, 126-130.

Avila-Flores, A., Rendón-Huerta, E., Moreno, J., Islas, S., Betanzos, A., Robles-Flores, M. and González-Mariscal, L. (2001). Tight-junction protein zonula occludens 2 is a target of phosphorylation by protein kinase C. *Biochem. J.* **360**, 295-304.

Balda, M. S., Whitney, J. A., Flores, C., González, S., Cereijido, M. and Matter, K. (1996). Functional dissociation of paracellular permeability and transepithelial electrical resistance and disruption of the apical-basolateral intramembrane diffusion barrier by expression of a mutant tight junction membrane protein. *J. Cell Biol.* **134**, 1031-1049.

Blanchard, A., Jeunemaitre, X., Coudol, P., Dechaux, M., Froissart, M., May, A., Demontis, R., Fournier, A., Paillard, M. and Houillier, P. (2001). Paracellin-1 is critical for magnesium and calcium reabsorption in the human thick ascending limb of Henle. *Kidney Int.* **59**, 2206-2215.

Colegio, O. R., Van Itallie, C., McCrea, H. J., Rahner, C. and Anderson, J. M. (2002). Claudin create charge-selective channels in the paracellular pathway between epithelial cells. *Am. J. Physiol. Cell Physiol.* **283**, C142-C147.

D'Souza, T., Agarwal, R. and Morin, P. J. (2005). Phosphorylation of claudin-3 at threonine 192 by PKA regulates tight junction barrier function in ovarian cancer cells. *J. Biol. Chem.* **280**, 26233-26240.

Dick, L. R., Cruikshank, A. A., Grenier, L., Melandri, F. D., Nunes, S. L. and Stein, R. L. (1996). Mechanistic studies on the inactivation of the proteasome by lactacystin: a central role for clasto-lactacystin beta-lactone. *J. Biol. Chem.* **271**, 7273-7276.

Fanning, A. S., Jameson, B. J., Jesaitis, L. A. and Anderson, J. M. (1998). The tight junction protein ZO-1 establishes a link between the transmembrane protein occludin and the actin cytoskeleton. *J. Biol. Chem.* **273**, 29745-29753.

Fujibe, M., Chiba, H., Kojima, T., Soma, T., Wada, T., Yamashita, T. and Sawada, N. (2004). Thr203 of claudin-1, a putative phosphorylation site for MAP kinase, is required to promote the barrier function of tight junctions. *Exp. Cell Res.* **295**, 36-47.

Furuse, M., Itoh, M., Hirase, T., Nagafuchi, A., Yonemura, S., Tsukita, S. and Tsukita, S. (1994). Direct association of occludin with ZO-1 and its possible involvement in the localization of occludin at tight junctions. *J. Cell Biol.* **127**, 1617-1626.

Gow, A., Southwood, C. M., Li, J. S., Pariali, M., Riordan, G. P., Brodie, S. E., Danias, J., Bronstein, J. M., Kachar, B. and Lazzarini, R. A. (1999). CNS myelin and sertoli cell tight junction strands are absent in Osp/claudin-11 null mice. *Saibo* **99**, 649-659.

Greger, R. (1985). Ion transport mechanisms in thick ascending limb if Henle's loop of mammalian nephron. *Physiol. Rev.* **65**, 760-797.

Hopkins, A. M., Walsh, S. V., Verkade, P., Boquet, P. and Nusrat, A. (2003). Constitutive activation of Rho proteins by CNF-1 influences tight junction structure and epithelial barrier function. *J. Cell Sci.* **116**, 725-742.

Hou, J., Paul, D. L. and Goodenough, D. A. (2005). Paracellin-1 and the modulation of ion selectivity of tight junctions. *J. Cell Sci.* **118**, 5109-5118.

Ikari, A., Hirai, N., Shiroma, M., Harada, H., Sakai, H., Hayashi, H., Suzuki, Y., Degawa, M. and Takagi, K. (2004). Association of paracellin-1 with ZO-1 augments the reabsorption of divalent cations in renal epithelial cells. *J. Biol. Chem.* **279**, 54826-54832.

Ishizaki, T., Chiba, H., Kojima, T., Fujibe, M., Soma, T., Miyajima, H., Nagasawa, K., Wada, I. and Sawada, N. (2003). Cyclic AMP induces phosphorylation of claudin-5 immunoprecipitates and expression of claudin-5 gene in blood-brain-barrier endothelial cells via protein kinase A-dependent and -independent pathways. *Exp. Cell Res.* **290**, 275-288.

Itoh, M., Nagafuchi, A., Moroi, S. and Tsukita, S. (1997). Involvement of ZO-1 in cadherin-based cell adhesion through its direct binding to alpha catenin and actin filaments. *J. Cell Biol.* **138**, 181-192.

Itoh, M., Furuse, M., Morita, K., Kubota, K., Saitou, M. and Tsukita, S. (1999a). Direct binding of three tight junction-associated MAGUKs, ZO-1, ZO-2, and ZO-3, with the COOH termini of claudins. *J. Cell Biol.* **147**, 1351-1363.

Itoh, M., Morita, K. and Tsukita, S. (1999b). Characterization of ZO-2 as a MAGUK family member associated with tight as well as adherens junctions with a binding affinity to occludin and alpha catenin. *J. Biol. Chem.* **274**, 5981-5986.

Kahle, K. T., Macgregor, G. G., Wilson, F. H., Van Hoek, A. N., Brown, D., Ardito, T., Kashgarian, M., Giebisch, G., Hebert, S. C., Boulpaep, E. L. et al. (2004). Paracellular Cl^- permeability is regulated by WNK4 kinase: insight into normal physiology and hypertension. *Proc. Natl. Acad. Sci. USA* **101**, 14877-14882.

Kale, G., Naren, A. P., Sheth, P. and Rao, R. K. (2003). Tyrosine phosphorylation of occludin attenuates its interactions with ZO-1, ZO-2, and ZO-3. *Biochem. Biophys. Res. Commun.* **302**, 324-329.

Karczewski, J. and Groot, J. (2000). Molecular physiology and pathophysiology of tight

junctions III. Tight junction regulation by intracellular messengers: differences in response within and between epithelia. *Am. J. Physiol. Gastrointest. Liver Physiol.* **279**, G660-G665.

Kimizuka, H. and Koketsu, K. (1964). Ion transport through cell membrane. *J. Theor. Biol.* **6**, 290-305.

Kiroytcheva, M., Cheval, L., Carranza, M. L., Martin, P. Y., Favre, H., Doucet, A. and Féraille, E. (1999). Effect of cAMP on the activity and the phosphorylation of Na^+,K^+-ATPase in rat thick ascending limb of Henle. *Kidney Int.* **55**, 1819-1831.

Leontieva, O. V. and Black, J. D. (2004). Identification of two distinct pathways of protein kinase Calpha down-regulation in intestinal epithelial cells. *J. Biol. Chem.* **279**, 5788-5801.

Mandon, B., Siga, E., Roinel, N. and de Rouffignac, C. (1993). Ca^{2+}, Mg^{2+} and K^+ transport in the cortical and medullary thick ascending limb of the rat nephron: influence of transepithelial voltage. *Pflugers Arch.* **424**, 558-560.

Marques, C., Pereira, P., Taylor, A., Liang, J. N., Reddy, V. N., Szweda, L. I. and Shang, F. (2004). Ubiquitin-dependent lysosomal degradation of the HNE-modified proteins in lens epithelial cells. *FASEB J.* **18**, 1424-1426.

McCarthy, K. M., Francis, S. A., McCormack, J. M., Lai, J., Rogers, R. A., Skare, I. B., Lynch, R. D. and Schneeberger, E. E. (2000). Inducible expression of claudin-1-myc but not occludin-VSV-G results in aberrant tight junction strand formation in MDCK cells. *J. Cell Sci.* **113**, 3387-3398.

Meade, P., Hoover, R. S., Plata, C., Vázquez, N., Bobadilla, N. A., Gamba, G. and Hebert, S. C. (2003). cAMP-dependent activation of the renal-specific Na^+-K^+-$2Cl^-$ cotransporter is mediated by regulation of cotransporter trafficking. *Am. J. Physiol. Renal Physiol.* **284**, F1145-F1154.

Mosesson, Y., Shtiegman, K., Katz, M., Zwang, Y., Vereb, G., Szollosi, J. and Yarden, Y. (2003). Endocytosis of receptor tyrosine kinases is driven by monoubiquitylation, not polyubiquitylation. *J. Biol. Chem.* **278**, 21323-21326.

Müller, D., Kausalya, P. J., Claverie-Martin, F., Meij, I. C., Eggert, P., Garcia-Nieto, V. and Hunziker, W. (2003). A novel claudin 16 mutation associated with childhood hypercalciuria abolishes binding to ZO-1 and results in lysosomal mistargeting. *Am. J. Hum. Genet.* **73**, 1293-1301.

Nakatsu, F., Sakuma, M., Matsuo, Y., Arase, H., Yamasaki, S., Nakamura, N., Saito, T. and Ohno, H. (2000). A Di-leucine signal in the ubiquitin moiety. Possible involvement in ubiquitination-mediated endocytosis. *J. Biol. Chem.* **275**, 26213-26219.

Nunbhakdi-Craig, V., Machleidt, T., Ogris, E., Bellotto, D., White, C. L. and Sontag, E. (2002). Protein phosphatase 2A associates with and regulates atypical PKC and the epithelial tight junction complex. *J. Cell Biol.* **158**, 967-978.

Nusrat, A., Parkos, C. A., Verkade, P., Foley, C. S., Liang, T. W., Innis-Whitehouse, W., Eastburn, K. K. and Madara, J. L. (2000a). Tight junctions are membrane microdomains. *J. Cell Sci.* **113**, 1771-1781.

Nusrat, A., Turner, J. R. and Madara, J. L. (2000b). Molecular physiology and pathophysiology of tight junctions. IV. Regulation of tight junctions by extracellular stimuli: nutrients, cytokines, and immune cells. *Am. J. Physiol. Gastrointest. Liver Physiol.* **279**, G851-G857.

Ohkuma, S., Chudzik, J. and Poole, B. (1986). The effects of basic substances and acidic ionophores on the digestion of exogenous and endogenous proteins in mouse peritoneal macrophages. *J. Cell Biol.* **102**, 959-966.

Quamme, G. A. (1989). Control of magnesium transport in the thick ascending limb. *Am. J. Physiol.* **256**, F197-F210.

Quamme, G. A. (1997). Renal magnesium handling: new insights in understanding old problems. *Kidney Int.* **52**, 1180-1195.

Quamme, G. A. and de Rouffignac, C. (2000). Epithelial magnesium transport and regulation by the kidney. *Front. Biosci.* **5**, D694-D711.

Simon, D. B., Lu, Y., Choate, K. A., Velazquez, H., Al-Sabban, E., Praga, M., Casari, G., Bettinelli, A., Colussi, G., Rodriguez-Soriano, J. et al. (1999). Paracellin-1, a renal tight junction protein required for paracellular Mg2+ resorption. *Science* **285**, 103-106.

Slatopolsky, E., Mercado, A., Morrison, A., Yates, J. and Klahr, S. (1976). Inhibitory effects of hypermagnesemia on the renal action of parathyroid hormone. *J. Clin. Invest.* **58**, 1273-1279.

Soma, T., Chiba, H., Kato-Mori, Y., Wada, T., Yamashita, T., Kojima, T. and Sawada, N. (2004). Thr(207) of claudin-5 is involved in size-selective loosening of the endothelial barrier by cyclic AMP. *Exp. Cell Res.* **300**, 202-212.

Srivastava, J., Procyk, K. J., Iturrioz, X. and Parker, P. J. (2002). Phosphorylation is required for PMA- and cell-cycle-induced degradation of protein kinase Cdelta. *Biochem. J.* **368**, 349-355.

Staehelin, L. A. (1974). Structure and function of intercellular junctions. *Int. Rev. Cytol.* **39**, 191-283.

Tasic, V., Dervisov, D., Koceva, S., Weber, S. and Konrad, M. (2005). Hypomagnesemia with hypercalciuria and nephrocalcinosis: case report and a family study. *Pediatr. Nephrol.* **20**, 1003-1006.

Tsukamoto, T. and Nigam, S. K. (1997). Tight junction proteins form large complexes and associate with the cytoskeleton in an ATP depletion model for reversible junction assembly. *J. Biol. Chem.* **272**, 16133-16139.

Tsukita, S., Furuse, M. and Itoh, M. (1999). Structural and signalling molecules come together at tight junctions. *Curr. Opin. Cell Biol.* **11**, 628-633.

Van Itallie, C., Rahner, C. and Anderson, J. M. (2001). Regulated expression of claudin-4 decreases paracellular conductance through a selective decrease in sodium permeability. *J. Clin. Invest.* **107**, 1319-1327.

Van Itallie, C. M., Fanning, A. S. and Anderson, J. M. (2003). Reversal of charge selectivity in cation or anion-selective epithelial lines by expression of different claudins. *Am. J. Physiol. Renal Physiol.* **285**, F1078-F1084.

Weber, S., Schlingmann, K. P., Peters, M., Nejsum, L. N., Nielsen, S., Engel, H., Grzeschik, K. H., Seyberth, H. W., Gröne, H. J., Nüsing, R. et al. (2001). Primary gene structure and expression studies of rodent paracellin-1. *J. Am. Soc. Nephrol.* **12**, 2664-2672.

Wilcox, E. R., Burton, Q. L., Naz, S., Riazuddin, S., Smith, T. N., Ploplis, B., Belyantseva, I., Ben-Yosef, T., Liburd, N. A., Morell, R. J. et al. (2001). Mutations in the gene encoding tight junction claudin-14 cause autosomal recessive deafness DFNB29. *Saibo* **104**, 165-172.

Wittchen, E. S., Haskins, J. and Stevenson, B. R. (1999). Protein interactions at the tight junction. Actin has multiple binding partners, and ZO-1 forms independent complexes with ZO-2 and ZO-3. *J. Biol. Chem.* **274**, 35179-35185.

Wittner, M. and Di Stefano, A. (1990). Effects of antidiuretic hormone, parathyroid hormone and glucagon on transepithelial voltage and resistance of the cortical and medullary thick ascending limb of Henle's loop of the mouse nephron. *Pflugers Arch.* **415**, 707-712.

Yamauchi, K., Rai, T., Kobayashi, K., Sohara, E., Suzuki, T., Itoh, T., Suda, S., Hayama, A., Sasaki, S. and Uchida, S. (2004). Disease-causing mutant WNK4 increases paracellular chloride permeability and phosphorylates claudins. *Proc. Natl. Acad. Sci. USA* **101**, 4690-4694.

Yu, A. S., Enck, A. H., Lencer, W. I. and Schneeberger, E. E. (2003). Claudin-8 expression in Madin-Darby canine kidney cells augments the paracellular barrier to cation permeation. *J. Biol. Chem.* **278**, 17350-17359.